

The properties of strange quark matter under strong rotation

Fei Sun^{1,2*} and Anping Huang^{2,3†}

¹*Department of Physics, China Three Gorges University, Yichang, 443002, China*

²*Physics Department and Center for Exploration of Energy and Matter, Indiana University, 2401 N Milo B. Sampson Lane, Bloomington, Indiana 47408, USA*

³*School of Nuclear Science and Technology, University of Chinese Academy of Sciences, Beijing 100049, China*

We investigate the rotating quark matter in the three-flavor Nambu and Jona-Lasinio (NJL) model. The chiral condensation, spin polarization and number susceptibility of strange quark are carefully studied at finite temperature without or with finite chemical potential in this model. We find that the rotation suppresses the chiral condensation and enhances the first-order quark spin polarization, however for the second-order quark spin polarization and quark number susceptibility the effect is very interesting, in the case of zero chemical potential which have a jump structure when the first-order phase transitions take place. When extending to the situation with finite chemical potential, we find the angular velocity also plays a crucial role, at small or large enough angular velocity the chemical potential enhances the susceptibility, however in the middle region of angular velocity the effect of the chemical potential is suppressed by the angular velocity and susceptibility can be changed considerably, which can be also observed that the quark number susceptibility has two maximum value. Furthermore, it is found that at sufficiently large angular velocity the contributions played by light quark and strange quark to these phenomena are almost equal. We expect these studies to be used to understand the chiral symmetry breaking and restoration as well as probe the QCD phase transition.

I. INTRODUCTION

QCD thermodynamics has always been the subject of intense investigations for many years, which motivates various works to try to understand it better, and we know many about the equation of state of strongly interacting matter as a function of temperature T and in a limited range of quark chemical potential μ . Recently, QCD matter under rotation is of particular interest, there exist some interesting phenomena in rotating QCD matter, such as chiral vortical effect or chiral vortical wave [1–4], which is a key ingredient in theories that predict observable effects associated with chiral symmetry restoration and the production of false QCD vacuum states [5]. Many works can be investigated in various rotation-related phenomena, such as noncentral heavy-ion collisions in high energy nuclear physics [6–14], the mesonic condensation of isospin matter with rotation in hadron physics [15], the trapped non-relativistic bosonic cold atoms in condensed matter physics [16–20], the rapidly spinning neutron stars in astrophysics [21–29]. Quark matter under rotation has been studied in ultra-relativistic heavy-ion off-central collisions performed at Relativistic Heavy Ion Collider (RHIC) or Large Hadron Collider (LHC) as well as lattice simulation. It is known that for the region with very low temperature and very large chemical potential there exist uncertainty in lattice QCD due to the “sign problem”, Ref. [30] has calculate the angular momenta of gluons and quarks in the rotating QCD vacuum, which would very important for future theoretical research.

One interesting phenomenon is the quark spin polarization in noncentral collisions of heavy ions, where quark-gluon plasma (QGP) can be generated. And the global quark polarization could occur in the QGP due to the large angular

momentum carried by two colliding nuclei, spin-orbit coupling can generate a spin alignment (polarization) along the direction of the system angular momentum. This polarization provides very valuable information about the QGP properties and can be measured experimentally with hyperons via parity-violating weak decays [31–42]. Experimental measurements of the Λ hyperon polarization has been investigated at RHIC and LHC, which would be very helpful in the study of the hottest, least viscous and most vortical-fluid ever produced both for the theoretical physics and experimental physics. Recently, the global spin polarization of Λ and $\bar{\Lambda}$ has been measured by the STAR collaboration in Au+Au collisions over a wide range of beam energies $\sqrt{s_{NN}} = 7.7 - 200$ GeV and by ALICE collaboration in Pb+Pb collisions at 2.76 TeV and 5.02 TeV [43–45]. On the other hand, theoretical research of spin polarization in the quark matter has been exploring [46–52], which plays an important role to explain the origin of strong magnetic field in the magnetar as well as in changing the dynamical mass and some other phenomenon related the chiral symmetric phase transition. It would be very interesting to take into account the influence of the rotating effect to the quark spin polarization, especially, in the case of s quark matter under rotation. The study of quark spin polarization which linked to the vorticity may help us understanding the vortical nature of QGP and the chiral dynamics of the system.

Another interesting phenomenon in non-central collisions of heavy ions is the fluctuations and correlations of conserved charges as quantified by the corresponding susceptibilities, which are sensitive observable quantity in relativistic heavy-ion collisions and also considered as a useful probe for QGP [53–63]. In this paper we mainly focus on the baryon number fluctuation which is also simply related the quark number susceptibility (QNS). QNS serves as a signature for the QGP formation in ultra relativistic heavy-ion collision and also plays an important factor to probe that the QCD phase transition as well as the equation of state (EOS) of strongly interacting matter [64–66]. Experimentally, various cumulants of net-kaon

* sunfei@ctgu.edu.cn

† huanganping@ucas.ac.cn

multiplicity distributions of Au+Au collisions at $\sqrt{s_{NN}} = 7.7 - 200$ GeV has been measured by the STAR experiment [67–69], which are related to the thermodynamic susceptibilities. The study of QNS in lattice QCD has been interesting [70–74]. Although susceptibilities have been studied in the past [75–78], it has not been checked what influence will be get if considering the contribution from the strange quark matter [79–90] in the rotation system.

In this paper, encouraged by the successful description of two-flavor QCD under rotation [91] in the Nambu-Jona-Lasinio (NJL) model, which embodies the spontaneous breaking of chiral symmetry via effective interactions between quarks, we further study the three-flavor NJL model in the framework of quark under rotation. Since there are several flavors and colors of quarks, several pairings are possible, which probably lead to a great variety of interesting phenomena. And the questions we are going to address are how the chiral condensate, quark spin polarization and quark number susceptibility are influenced by the rotation.

Our work is organized as follows. We first discuss the formalism of three-flavor NJL model in the presence of rotation in Section II, by using mean-field approach and the finite temperature field methods we obtain the grand potential of the fermions with rotating, and the corresponding analytical ex-

pressions for the gap equation, spin polarization and susceptibility of the quarks are given. Section III presents numerical results and discussions in detail. Section IV summarizes and concludes the paper. A brief description of fermions under rotation is given in Appendix A, which discuss the complete set of commuting operators in cylindrical coordinates and derive the eigenstates of these operators.

II. FORMALISM

We start from the NJL model, the simplest three-flavor NJL Lagrangian for fermions without rotation is given by [92]

$$\mathcal{L} = \bar{\psi} (i\partial_\mu \gamma^\mu - m) \psi + G \sum_{a=0}^8 (\bar{\psi} \lambda^a \psi)^2, \quad (1)$$

here the $\lambda^a (a = 1, \dots, 8)$ are the Gell-Mann matrices in flavor space with

$$\lambda^0 = \sqrt{\frac{2}{3}} \begin{pmatrix} 1 & 0 & 0 \\ 0 & 1 & 0 \\ 0 & 0 & 1 \end{pmatrix}. \quad (2)$$

Using the mean field approximation which means that fluctuations are assumed to be small, the chiral condensates $\langle \bar{\psi}_i \psi_j \rangle$ with $i \neq j$ vanishes since it is assumed that flavor is conserved and after expanding the operators around their expectation values and neglecting the higher order fluctuations, we obtain

$$(\bar{\psi}_i \psi_j)^2 = -\langle \bar{\psi}_i \psi_j \rangle^2 + 2 \langle \bar{\psi}_i \psi_j \rangle \bar{\psi}_i \psi_j, (i = j), \quad (3)$$

and the Lagrangian can reads

$$\mathcal{L} = \bar{u} (i\partial_\mu \gamma^\mu - M_u) u + \bar{d} (i\partial_\mu \gamma^\mu - M_d) d + \bar{s} (i\partial_\mu \gamma^\mu - M_s) s - 2G \left(\langle \bar{u}u \rangle^2 + \langle \bar{d}d \rangle^2 + \langle \bar{s}s \rangle^2 \right), \quad (4)$$

where we have defined the dynamical quark mass M as follows

$$M_u = m_u - 4G \langle \bar{u}u \rangle; M_d = m_d - 4G \langle \bar{d}d \rangle; M_s = m_s - 4G \langle \bar{s}s \rangle, \quad (5)$$

finally, the three-flavor NJL Lagrangian for fermions reads

$$\mathcal{L} = \bar{u} (i\partial_\mu \gamma^\mu - M_u) u + \bar{d} (i\partial_\mu \gamma^\mu - M_d) d + \bar{s} (i\partial_\mu \gamma^\mu - M_s) s - \left(\frac{(M_u - m_u)^2}{8G} + \frac{(M_d - m_d)^2}{8G} + \frac{(M_s - m_s)^2}{8G} \right). \quad (6)$$

The general definition of the partition function can be written as

$$\mathcal{Z} = \int D[\bar{\psi}] D[\psi] e^{iS}, \quad (7)$$

here, S denotes the quark action, which is the integration of the Lagrangian density \mathcal{L} , then

$$\mathcal{Z} = \int D[\bar{\psi}] D[\psi] e^{i \int d^4x \left(\bar{\psi} (i\gamma^\mu \partial_\mu - m) \psi + G \sum_{a=0}^8 (\bar{\psi} \lambda^a \psi)^2 \right)}. \quad (8)$$

The Lagrangian of the rotating fermions which considering nonzero chemical potential can be written in the following way

$$\mathcal{L} = \bar{\psi} \left[i\gamma^\mu \partial_\mu - m + \gamma^0 \mu + (\gamma^0)^{-1} \left((\vec{\omega} \times \vec{x}) \cdot (-i\vec{\partial}) + \vec{\omega} \cdot \vec{S}_{4 \times 4} \right) \right] \psi + G \sum_{a=0}^8 (\bar{\psi} \lambda^a \psi)^2, \quad (9)$$

where ψ is the quark field, ω is the angular velocity and m is the bare quark mass matrix, as a result of rotation we can see the Dirac operator includes the orbit-rotation coupling term and the spin-rotation coupling term. After carrying out the general approach of the path integral formulation for Grassmann variables, we are now able to exactly integrate out the fermionic fields and we obtain

$$\log \mathcal{Z} = -\frac{1}{T} \int d^3x \left(\frac{(M_u - m_u)^2}{8G} + \frac{(M_d - m_d)^2}{8G} + \frac{(M_s - m_s)^2}{8G} \right) + \log \det \frac{D_u^{-1}}{T} + \log \det \frac{D_d^{-1}}{T} + \log \det \frac{D_s^{-1}}{T}, \quad (10)$$

here

$$D_u^{-1} = \gamma^0 \left(-i\omega_l u + \left(n + \frac{1}{2} \right) \omega + \mu_u \right) - M_u - \vec{\gamma} \cdot \vec{p}_u \quad (11)$$

is the inverse of propagator for u quark, similarly expressions can be obtained for D_d^{-1} and D_s^{-1} , and

$$\log \det \frac{\hat{D}^{-1}}{T} = \text{tr} \log \frac{\hat{D}^{-1}}{T} = \int d^3x \int \frac{d^3p}{(2\pi)^3} \langle \psi_p(x) | \log \hat{D}^{-1} | \psi_p(x) \rangle. \quad (12)$$

The Dirac fields can be defined in the terms of the wave functions $u(x), v(x)$

$$\psi_p(x) = \sum_{E,n,s,p} (u(x) + v(x)), \quad (13)$$

by substituting this expression, the above expression becomes

$$\log \det \frac{\hat{D}^{-1}}{T} = \sum_{E,n,s,p} \text{tr} \log \frac{D_{u(x)}^{-1}}{T} \int d^3x \int \frac{d^3p}{(2\pi)^3} (\langle u(x) | u(x) \rangle) \quad (14)$$

$$+ \sum_{E,n,s,p} \text{tr} \log \frac{D_{v(x)}^{-1}}{T} \int d^3x \int \frac{d^3p}{(2\pi)^3} (\langle v(x) | v(x) \rangle), \quad (15)$$

here, the concrete form of the D_u^{-1} that has considered the rotation is

$$D_{u(x)}^{-1} = \begin{pmatrix} (-i\omega_l + (n + \frac{1}{2})\omega + \mu) - M & -\vec{\sigma} \cdot \vec{p} \\ \vec{\sigma} \cdot \vec{p} & (-i\omega_l + (n + \frac{1}{2})\omega + \mu) - M \end{pmatrix}, \quad (16)$$

which corresponding to the positive energy solution, and the concrete form for the D_v^{-1} is

$$D_{v(x)}^{-1} = \begin{pmatrix} (i\omega_l - (n + \frac{1}{2})\omega + \mu) - M & -\vec{\sigma} \cdot \vec{p} \\ \vec{\sigma} \cdot \vec{p} & (i\omega_l - (n + \frac{1}{2})\omega + \mu) - M \end{pmatrix}, \quad (17)$$

which corresponding to the negative energy solution. Here, in order to study the rotating system at finite density, we have introduced quark chemical potential μ and note that the term $(n + \frac{1}{2})\omega$ in above expressions denotes the rotational polarization energy, which are very useful when we study the polarization in the following sections. By using the general methods in the finite temperature fields [93], we obtain

$$\begin{aligned} \log \det \frac{D_u^{-1}}{T} = & \beta \left(\sqrt{M^2 + p_t^2 + p_z^2} + (n + \frac{1}{2})\omega \right) \\ & + \log \left(e^{\beta(\sqrt{M^2 + p_t^2 + p_z^2} + ((n + \frac{1}{2})\omega - \mu))} + 1 \right) \\ & + \log \left(e^{\beta(\sqrt{M^2 + p_t^2 + p_z^2} + ((n + \frac{1}{2})\omega + \mu))} + 1 \right), \end{aligned} \quad (18)$$

and

$$\begin{aligned} \log \det \frac{D_v^{-1}}{T} = & \beta \left(-\sqrt{M^2 + p_t^2 + p_z^2} - (n + \frac{1}{2})\omega \right) \\ & + \log \left(e^{\beta(-\sqrt{M^2 + p_t^2 + p_z^2} - ((n + \frac{1}{2})\omega - \mu))} + 1 \right) \\ & + \log \left(e^{\beta(-\sqrt{M^2 + p_t^2 + p_z^2} - ((n + \frac{1}{2})\omega + \mu))} + 1 \right). \end{aligned} \quad (19)$$

Here β is the inverse temperature and the inner products of $\langle u_{n,s} | u_{n,s} \rangle$, $\langle v_{n,s} | v_{n,s} \rangle$ are derived with very simple expressions as follows,

$$\int \frac{d^3 p}{(2\pi)^3} \langle u_{n,s} | u_{n,s} \rangle = \frac{1}{2} \left(J_n(p_t r)^2 + J_{n+1}(p_t r)^2 \right), \quad (20)$$

$$\int \frac{d^3 p}{(2\pi)^3} \langle v_{n,s} | v_{n,s} \rangle = \frac{1}{2} \left(J_n(p_t r)^2 + J_{n+1}(p_t r)^2 \right). \quad (21)$$

Combining the Eqs. (10), (18), (19), (20) and (21) one could now derive the expression of the grand potential for strange quark when the momentum summation turns into the integration

$$\sum_p \rightarrow V \int \frac{d^3 p}{(2\pi)^3}, \quad (22)$$

and the energy summation performs over Matsubara frequency. Then the thermodynamic grand potential $\Omega = -T \log \mathcal{Z}$ have the following expression,

$$\begin{aligned} \Omega = & \frac{(M-m)^2}{8G} - \frac{3}{16\pi^2} \sum_{n=-\infty}^{\infty} \int_0^{\Lambda} p_t dp_t \int_0^{2\pi} \sin \theta d\theta \int_{-\sqrt{\Lambda^2 - p_t^2}}^{\sqrt{\Lambda^2 - p_t^2}} dp_z \left((J_{n+1}(p_t r)^2 + J_n(p_t r)^2) \right. \\ & T \left\{ \log \left(e^{-\frac{-\mu + \sqrt{M^2 + p_t^2 + p_z^2} - (n + \frac{1}{2})\omega}{T}} + 1 \right) + \log \left(e^{-\frac{-\mu + \sqrt{M^2 + p_t^2 + p_z^2} - (n + \frac{1}{2})\omega}{T}} + 1 \right) \right. \\ & \left. \left. + \log \left(e^{-\frac{\mu + \sqrt{M^2 + p_t^2 + p_z^2} - (n + \frac{1}{2})\omega}{T}} + 1 \right) + \log \left(e^{\frac{\mu + \sqrt{M^2 + p_t^2 + p_z^2} - (n + \frac{1}{2})\omega}{T}} + 1 \right) \right\}. \right) \end{aligned} \quad (23)$$

Here, the Λ is the three-momentum cutoff which should be chosen to reproduce observables of the pion and so on, also, the isospin and color degrees of freedom give factor 2 and 3 have been considered, respectively.

We have discussed the evaluating of grand potential of quark under rotation in detail in the previous section. In this section, we list our final analytical expressions of the gap

equation, quark spin polarization and quark number susceptibility in the situation with rotation. Firstly, we consider the gap equation which will be required to minimize the grand potential, the values are determined by solving the stationary condition, namely, $\frac{\partial \Omega}{\partial M} = 0$, $\frac{\partial^2 \Omega}{\partial M^2} > 0$, and the detailed expressions are listed as follows,

$$\begin{aligned} \frac{\partial \Omega}{\partial M} = & \frac{(M-m)}{4G} - \frac{3}{16\pi^2} \sum_{n=-\infty}^{\infty} \int_0^{\Lambda} p_t dp_t \int_0^{2\pi} \sin \theta d\theta \int_{-\sqrt{\Lambda^2 - p_t^2}}^{\sqrt{\Lambda^2 - p_t^2}} dp_z \left((J_{n+1}(p_t r)^2 + J_n(p_t r)^2) \times \right. \\ & T \left(-\frac{2M \sinh \left(\frac{-2\sqrt{M^2 + p_t^2 + p_z^2} + 2n\omega + \omega}{2T} \right)}{T \sqrt{M^2 + p_t^2 + p_z^2} \left(\cosh \left(\frac{-2\sqrt{M^2 + p_t^2 + p_z^2} + 2n\omega + \omega}{2T} \right) + \cosh \left(\frac{\mu}{T} \right) \right)} \right), \end{aligned} \quad (24)$$

$$\begin{aligned}
\frac{\partial^2 \Omega}{\partial M^2} = & \frac{1}{4G} - \frac{3}{16\pi^2} \sum_{n=-\infty}^{\infty} \int_0^{\Lambda} p_t dp_t \int_0^{2\pi} \sin \theta d\theta \int_{-\sqrt{\Lambda^2 - p_t^2}}^{\sqrt{\Lambda^2 - p_t^2}} dp_z ((J_{n+1}(p_t r)^2 + J_n(p_t r)^2) \times \\
& T \left\{ \frac{2M^2 \cosh \left(\frac{-2\sqrt{M^2 + p_t^2 + p_z^2} + 2n\omega + \omega}{2T} \right)}{T^2(M^2 + p_t^2 + p_z^2) \left(\cosh \left(\frac{-2\sqrt{M^2 + p_t^2 + p_z^2} + 2n\omega + \omega}{2T} \right) + \cosh \left(\frac{\mu}{T} \right) \right)} \right. \\
& - \frac{2M^2 \sinh^2 \left(\frac{-2\sqrt{M^2 + p_t^2 + p_z^2} + 2n\omega + \omega}{2T} \right)}{T^2(M^2 + p_t^2 + p_z^2) \left(\cosh \left(\frac{-2\sqrt{M^2 + p_t^2 + p_z^2} + 2n\omega + \omega}{2T} \right) + \cosh \left(\frac{\mu}{T} \right) \right)^2} \\
& + \frac{2M^2 \sinh \left(\frac{-2\sqrt{M^2 + p_t^2 + p_z^2} + 2n\omega + \omega}{2T} \right)}{T(M^2 + p_t^2 + p_z^2)^{3/2} \left(\cosh \left(\frac{-2\sqrt{M^2 + p_t^2 + p_z^2} + 2n\omega + \omega}{2T} \right) + \cosh \left(\frac{\mu}{T} \right) \right)} \\
& - \left. \frac{2 \sinh \left(\frac{-2\sqrt{M^2 + p_t^2 + p_z^2} + 2n\omega + \omega}{2T} \right)}{T \sqrt{M^2 + p_t^2 + p_z^2} \left(\cosh \left(\frac{-2\sqrt{M^2 + p_t^2 + p_z^2} + 2n\omega + \omega}{2T} \right) + \cosh \left(\frac{\mu}{T} \right) \right)} \right\}. \tag{25}
\end{aligned}$$

Here we are going to study the quark spin polarization which can be defined as taking the partial derivative of minus grand potential with respect to angular velocity, and we

introduce the following quark spin polarization as in Ref. [94]

$$\mathcal{P}^1 = \frac{\partial(\frac{-\Omega}{T^4})}{\partial(\frac{\omega}{T})}, \tag{26}$$

$$\mathcal{P}^2 = \frac{\partial^2(\frac{-\Omega}{T^4})}{\partial(\frac{\omega}{T})^2}, \tag{27}$$

such definition ensures dimensionless polarization, then we list the detailed expression of the first-order polarization and second-order polarization as follows,

$$\begin{aligned}
\mathcal{P}^1 = & \frac{3}{16\pi^2} \sum_{n=-\infty}^{\infty} \int_0^{\Lambda} p_t dp_t \int_0^{2\pi} \sin \theta d\theta \int_{-\sqrt{\Lambda^2 - p_t^2}}^{\sqrt{\Lambda^2 - p_t^2}} dp_z ((J_{n+1}(p_t r)^2 + J_n(p_t r)^2) \times \\
& \frac{(2n+1) \sinh \left(\frac{-2\sqrt{M^2 + p_t^2 + p_z^2} + 2n\omega + \omega}{2T} \right)}{T \left(\cosh \left(\frac{-2\sqrt{M^2 + p_t^2 + p_z^2} + 2n\omega + \omega}{2T} \right) + \cosh \left(\frac{\mu}{T} \right) \right)}. \tag{28}
\end{aligned}$$

$$\begin{aligned}
\mathcal{P}^2 = & \frac{3}{16\pi^2} \sum_{n=-\infty}^{\infty} \int_0^{\Lambda} p_t dp_t \int_0^{2\pi} \sin \theta d\theta \int_{-\sqrt{\Lambda^2 - p_t^2}}^{\sqrt{\Lambda^2 - p_t^2}} dp_z ((J_{n+1}(p_t r)^2 + J_n(p_t r)^2) \times \\
& \frac{(2n+1)^2}{8T^2} \left(\operatorname{sech}^2 \left(\frac{2\mu - 2\sqrt{M^2 + p_t^2 + p_z^2} + 2n\omega + \omega}{4T} \right) + \operatorname{sech}^2 \left(\frac{-2\mu - 2\sqrt{M^2 + p_t^2 + p_z^2} + 2n\omega + \omega}{4T} \right) \right). \tag{29}
\end{aligned}$$

Next, we will investigate how much the rotation affects the baryon number fluctuations, these fluctuations can be quantified by the susceptibilities and the QNS is defined through the Taylor expansion coefficients of the pressure over the chemi-

cal potential [95–101]:

$$\chi_n = \frac{\partial^n(\frac{P}{T^4})}{\partial(\frac{\mu}{T})^n}, \tag{30}$$

here we focus on the second order derivative of pressure with respect to μ , due to symmetry all the odd susceptibilities van-

ishes when $\mu \rightarrow 0$ (note, in the context of lattice calculations the susceptibilities are often defined as dimensionless quanti-

ties), using the relation of pressure $P = -\Omega$, the actual calculation of the susceptibilities is straightforward and the detailed result is

$$\frac{\partial(-\Omega)}{\partial\mu} = \frac{3}{16\pi^2} \sum_{n=-\infty}^{\infty} \int_0^{\Lambda} p_t dp_t \int_0^{2\pi} \sin\theta d\theta \int_{-\sqrt{\Lambda^2-p_t^2}}^{\sqrt{\Lambda^2-p_t^2}} dp_z ((J_{n+1}(p_t r)^2 + J_n(p_t r)^2) \times$$

$$\frac{2 \sinh(\frac{\mu}{T})}{T \left(\cosh\left(\frac{-2\sqrt{M^2+p_t^2+p_z^2+2n\omega+\omega}}{2T}\right) + \cosh(\frac{\mu}{T}) \right)}, \quad (31)$$

and

$$\chi_2 = \frac{3}{16\pi^2} \sum_{n=-\infty}^{\infty} \int_0^{\Lambda} p_t dp_t \int_0^{2\pi} \sin\theta d\theta \int_{-\sqrt{\Lambda^2-p_t^2}}^{\sqrt{\Lambda^2-p_t^2}} dp_z ((J_{n+1}(p_t r)^2 + J_n(p_t r)^2) \times$$

$$\frac{1}{2T^2} \left(\operatorname{sech}^2\left(\frac{2\mu-2\sqrt{M^2+p_t^2+p_z^2+2n\omega+\omega}}{4T}\right) + \operatorname{sech}^2\left(\frac{-2\mu-2\sqrt{M^2+p_t^2+p_z^2+2n\omega+\omega}}{4T}\right) \right). \quad (32)$$

With the analytical expressions given above, we show our numerical results in the next section.

III. NUMERICAL RESULTS AND DISCUSSIONS

In this section we will present our numerical results for the the gap equation, quark spin polarization and quark number susceptibility. In our previous analytic expressions, the z -angular-momentum quantum number $n = 0, \pm 1, \pm 2, \dots$ in principle we should sum all the values of n , fortunately, these expressions converge so fast that it is enough for us to sum n from -5 to 5 , it should be noted that in order that the causality of a rigidly rotating system is maintained we should make sure that the local velocity is smaller than the light velocity, namely, the condition $\omega r < 1$ should be considered in all the calculations, and for simplicity we take the same value of r as in Ref. [91]. Since any uniformly rotating system should be spatially bounded, it has been expected that the presence of boundaries can modify the properties of the rotating system [102–106], indeed, this is only true when the angular velocity ω is much smaller than the inverse of the system's size [107] as well as our discussion is mainly devoted to the bulk properties of rotating system, so in our analytic derivation we ignore the finite volume boundary effect and we leave it as our further study. In our calculations, the input parameters in the NJL are the coupling constants G , the quark masses $m_{u/d}, m_s$ and the three-momentum cutoff Λ . We use the model parameters reported in Ref. [108] unless a particular specification being made, which have been estimated by the fitting in light of the following observations: $m_\pi = 138$ MeV, $f_\pi = 92$ MeV, $m_K = 495$ MeV and $m_{\eta'} = 958$ MeV. Our model is the simplest three-flavor NJL model which do not consider the contribution of the 't Hooft interaction, so in the case of a vanishing κ the parameters in Ref. [108] have been readjusted, keeping the values of Λ and m_u fixed and varying G

and m_s to obtain the same dressed masses estimated at zero temperature and density for the situation with $\kappa \neq 0$. Then, in this context, we worked with the following set

$$\begin{aligned} m_u &= m_d = 0.005 \text{ GeV}, \\ m_s &= 0.1 \text{ GeV}, \\ G &= 4.35 \text{ GeV}^{-2}, \\ \Lambda &= 0.68 \text{ GeV}. \end{aligned} \quad (33)$$

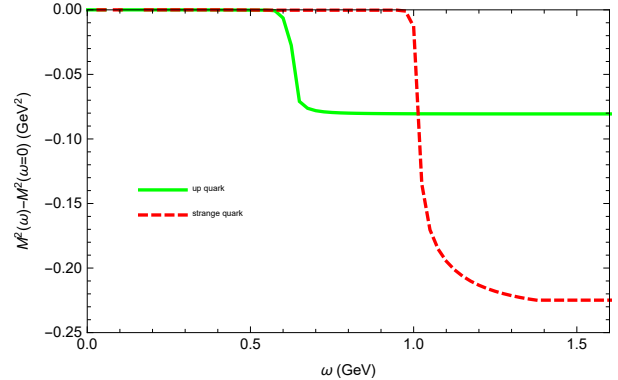


FIG. 1. (Color online) Differences of squared gap masses between the case at $\omega \neq 0$ and $\omega = 0$ with both $\mu = 0$ and $T = 0$ for up quark and strange quark as a function of ω .

Let us first discuss the results at chemical potential equals zero. We investigate the chiral condensation in rotating matter under the three-flavor NJL model, especially we consider the contribution from s quark. It is equivalent to study the gap equations since the gap equations correspond to the coupling of the quarks naked masses with the associated chiral condensates, firstly, in the plot of Fig. 1, we show the differences of squared gap masses between the case at nonzero angular velocity to those at zero angular velocity, $M^2(\omega) - M^2(\omega = 0)$

with zero temperature and zero chemical potential for the up quark and strange quark, respectively, we found that the squared gap mass differences of all quarks decrease with increasing angular velocity, and at large angular velocity there is a suddenly drop down for the squared gap mass differences, it obvious that the squared gap mass differences of lighter quark is more effected by the angular velocity, which decreases faster while that of strange quark decreases slower with angular velocity, this could partly due to that the quark with large current mass is less affected by the rotation. Then we plot the gap equation as a function of ω with different values of T in Fig. 2 respectively for u and s quark. As one can see, both u quark and s quark gap equations show that the rotation has a suppression effect for the chiral condensation. It is clearly seen that at all temperatures the gap equations of both u and s decrease with increasing ω and at very low temperature the chiral condensate experiences a first-order transition when ω exceeds a certain value. When comparing the different flavor situation, we find that for the first-order transition

of s quark we need larger values of ω compares to that of u , at $T = 0.01$ GeV in the left panel of Fig. 2 shows that M_u experiences a first-order transition around $\omega = 0.6$ GeV while in the right panel of Fig. 2 shows M_s experiences a first-order transition around $\omega = 1.0$ GeV. From the figure we can see the role of the ω as well as T are very important parameters for crossover or first-order transition. For the high temperatures the chiral condensate vanishes with the increasing ω via a smooth crossover, and the temperature effect becomes weak with increasing the value of ω . As ω further increases the gap equations for the both decrease more slowly, and both approach their naked masses. This can be interpreted as a hint that the chiral phase transitions for the s, u do not occur at the same angular velocity with the same temperature. It is found that the chiral condensation of u quark has produced results almost in agreement with those suggested in literature [4], but with a slightly difference due to they adopted the parameters in Ref. [109].

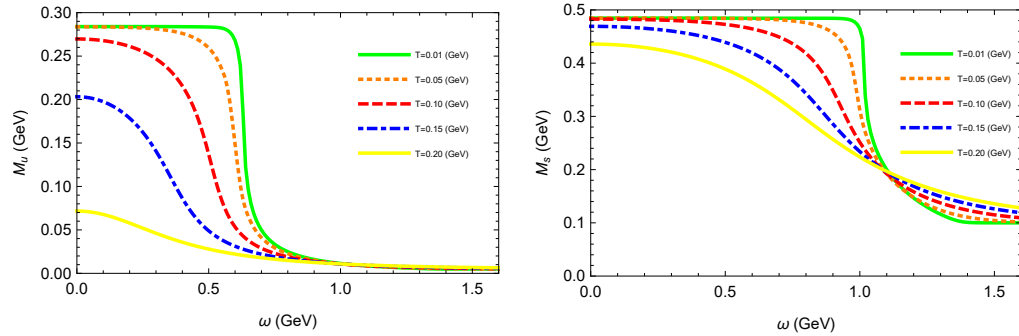


FIG. 2. (Color online) The mean field mass gap M_u and M_s as a function of ω for several values of T with $\mu = 0$.

We now turn to a more realistic physical environment, in Fig. 3 we plot the gap equation as a function of T with fixed angular velocity ω and radius r for u and s quark, respectively. In order to enable a more realistic comparison to experimental data in the future, here without losing generality, we assume that $\omega = 0.01, 0.1$ GeV and $r = 1, 1.6$ fm. From the figure we can see clearly that there exist some interesting behaviours in the range of $T = 0.1 \sim 0.4$ GeV. The left hand side of the Fig. 3 shows that the u quark gap mass decreases with increasing temperature, the mass gap M_u falls sharply in the range of $T = 0.15 \sim 0.2$ GeV, which means that at low T and small ω the quark condensate experiences a first-order transition when the temperature exceeds a certain value of critical

T_c . The right hand side of the Fig. 3 shows that for the chosen parameters the s quark gap mass decreases with increasing temperature via a crossover transition and the chiral condensate gradually vanishes with increasing temperature. From the left hand side of the Fig. 3 one can also see clearly that, for a fixed value of r the effect of rotation suppresses the critical temperature and for a fixed value of small ω we can observe that the transition temperature becomes smaller at larger radius. Here we just want to capture the essential physics of QCD matter under rotation, indeed, in realistic physical environment requires a more detailed investigation.

The first-order spin polarizations of u quark and s quark as a function of ω for several temperatures with chemical po-

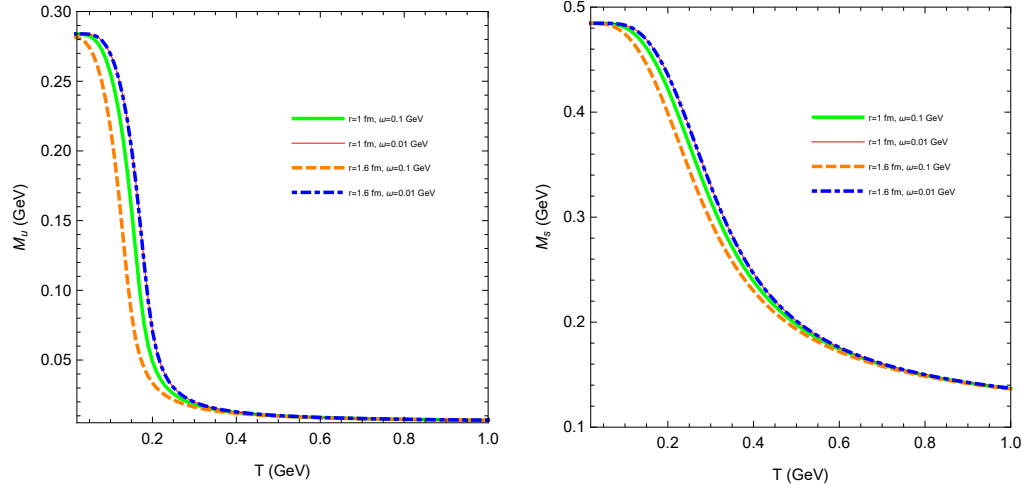


FIG. 3. (Color online) The mean field mass gap M_u and M_s as a function of T for several values of r and ω with $\mu = 0$.

tential equals zero are showed in Fig. 4, to be clear, the result of $T = 0.01$ GeV is divided by 100. It is very clear to see that the angular velocity has a strong influence on the quark first-order spin polarization as well as the temperature is also important to the polarization of the quark. From the figure it is observed that the rotation system may induce a large polarization both for u and s quark. At all temperatures the quark spin polarization increases with increasing angular velocity for all quarks. At low temperature the quark first-order spin polarization increases very rapidly in a certain angular velocity window and then increases very slowly, while at high temperature the quark first-order spin polarization increases almost linearly. Although the rotation affects all quarks, and Fig. 4 gives similar results for first-order spin polarizations of u quark and s quark, however there are some differences between them, next we will try to compare their own characteristics. An interesting feature worth to mention is that at low temperature for u quark spin polarization the angular velocity

enhance effect is manifest whereas for s quark spin polarization the enhance effect is not so manifest, until the angular velocity exceeds a certain value. And at very low temperature an interesting phenomenon of the jump of the quark first-order spin polarization can be observed around $\omega \sim 0.6$ GeV for u quark and around $\omega \sim 1.0$ GeV for s quark in Fig. 4, which is a hint for the first-order phase transition to occur. Another information should be noted is that at low ω , the polarization of u quark is easier to be achieved than that of s quark, however, with further increasing ω and when it exceeds a certain value, the polarization of both u and s quark show a very similar behavior each other. This indicates that at sufficiently large angular velocity, the part played by the different current quark masses in the spin polarization is very weak, however, at low angular velocity the part played by current mass is important. These distinguishing feature for the spin polarization of u and s may provide valuable insights for predicting the polarization in experiments.

In order to have a better understanding for the spin polarization of quark with rotation, we plot the second-order polarizations of the u and s quark as a function of ω for several temperatures with the chemical potential equals zero in Fig. 5. In the case of the temperature is very low, the spin polarization begins to occur at a certain value of the angular velocity and increasing with the angular velocity increases, until

it reaches the highest value, when the angular velocity is increased further, the spin polarization becomes weaker and finally disappears, the reason why the second-order quark spin polarization disappears at large angular velocity is that when the angular velocity becomes larger, the dynamical mass of the quark becomes smaller and the chiral symmetry is gradually restored so that the second-order quark spin polarization does not occur.

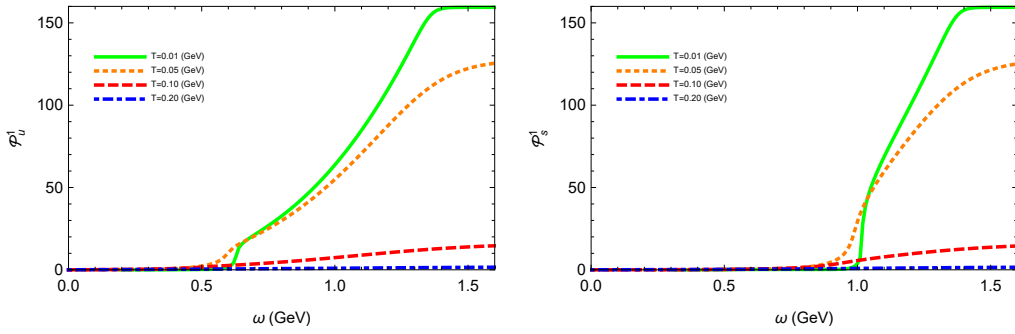


FIG. 4. (Color online) Study of the first-order polarizations \mathcal{P}^1 of the u and s quark according to ω for several temperature T with $\mu = 0$, here the result of $T = 0.01$ GeV is divided by 100.

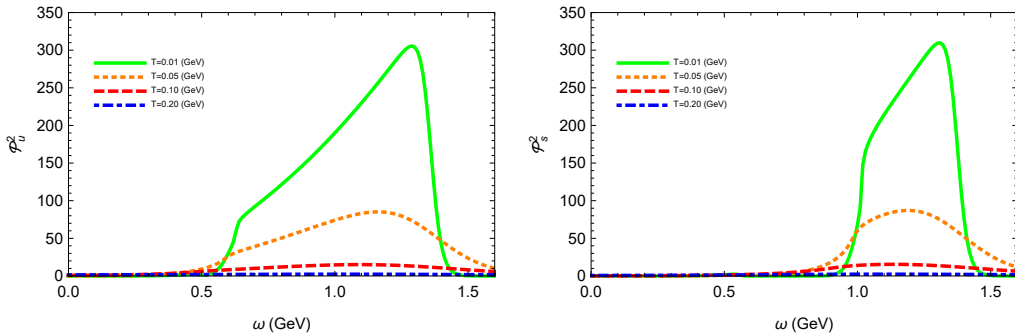


FIG. 5. (Color online) Study of the second-order polarizations of the u and s quark according to ω for several temperature T with $\mu = 0$.

On the other hand, in order to understand the equation of state under the rotation system better, it is helpful to study the behavior of baryon number susceptibility. We now turn to study the QNS and take into account the influence of angular velocity on QNS. Firstly, we consider the case of zero chemical potential, in Fig. 6 we plot the susceptibilities of u and s quark as a function of angular velocity for several fixed values of temperatures with zero chemical potential, to be clear, the result of $T = 0.01$ GeV is divided by 10. It is evident from the figure that the susceptibilities of u and s quark increase as the ω increases when ω is smaller than a certain value for all the temperatures while the susceptibilities decrease as the ω increases when ω is larger than another certain value. And it also can be seen from the figure the tem-

perature and the angular velocity play an important role in the susceptibility, at low temperature the quark chiral symmetry is broken spontaneously, however with the increasing of the angular velocity the chiral symmetry is restored, so we can see at low temperature and low angular velocity the susceptibility is very small and at low temperature and large angular velocity the susceptibility disappears, however if the temperature is high the susceptibility always occurs and the angular velocity plays a slightly effect on the rotating matter.

It is fairly clear that the susceptibility is a finite quantity that is furthermore sensitive to the mass of the quark, so next we will discuss the differences of the u and s quark number susceptibilities under the rotation. When angular velocity is small and temperature is high we find that susceptibil-

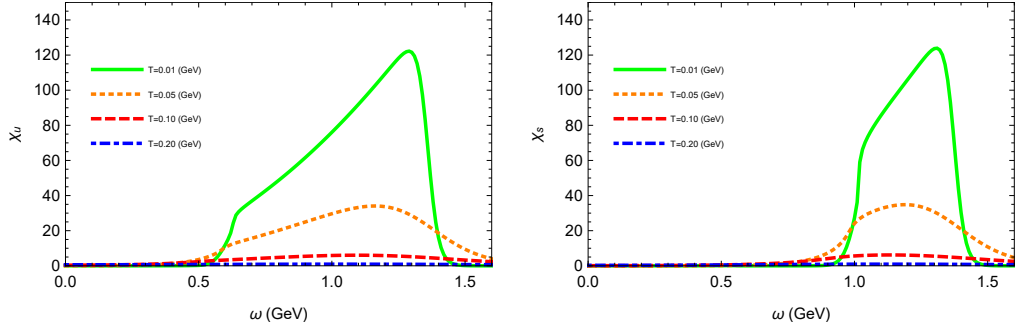


FIG. 6. (Color online) Susceptibilities of u and s quark as a function of ω for several values of T with $\mu = 0$, here the result of $T = 0.01$ GeV is divided by 10.

ity of u is larger than the susceptibility of s and when angular velocity and temperature are both small we find that it is easy for the susceptibility of u quark to occur, for instance, at $T = 0.01$ GeV, the u quark number susceptibility starts to occur at $\omega = 0.5$ GeV while for s quark number susceptibility starts to occur at $\omega = 0.9$ GeV. As we can see from the figure that the curves have the highest values only for some certain regions of the angular velocity, and at low temperature we find that there exist a narrower region obvious changes the QNS when comparing that of s quark with that of u quark at $T = 0.01$ GeV, it is clearly can be seen from the curves that

QNS changes little when the angular velocity is changed below 0.9 GeV or above 1.5 GeV for the s quark, however for that of u quark the angular velocity is below 0.5 GeV or above 1.5 GeV. It is very clear from the figure that the contribution from the angular velocity becomes dominant when $\omega \geq 1.1$ and the peaks of the susceptibilities appear at almost the same angular velocity. At all values of the chemical potential the behaviors of the u quark and s quark number susceptibility are very similar with increasing the angular velocity reveal that when the angular velocity is large the role played by the mass of different quarks becoming weaker and weaker and finally almost can be ignored.

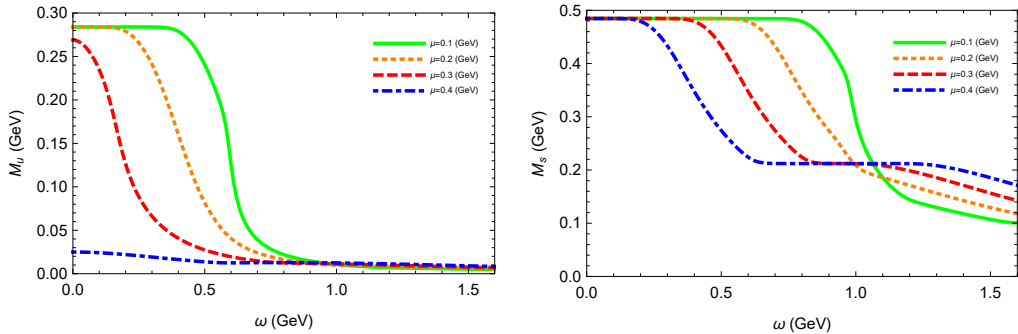


FIG. 7. (Color online) The mean field mass gap of u and s quark as a function of ω for several fixed values of μ at $T = 0.01$ GeV.

Let us now discuss the behavior of mean field mass gap of the quark at very low temperature with nonzero chemical potential, in Fig. 7 we plot M_u and M_s as a function of ω for a variety of values of μ at $T = 0.01$ GeV, respectively. Comparing with the Fig. 2, it is clear that a nonzero value of the chemical potential affects the first-order phase transition, at $T = 0.01$ GeV, there does not exist a sudden drop for the mean field mass gap when $\mu \neq 0$ both for u and s

quark, which indicating there exists a suppression effect for the chemical potential on the phase transition. At large chemical potential the chiral condensate vanishes with increasing ω via a smooth crossover. From the figure we can also see that there is a different behavior between u and d quark, the u quark is more affected by the presence of the chemical potential and angular velocity than s quark because the s quark has a substantial mass even after the chiral phase transition.

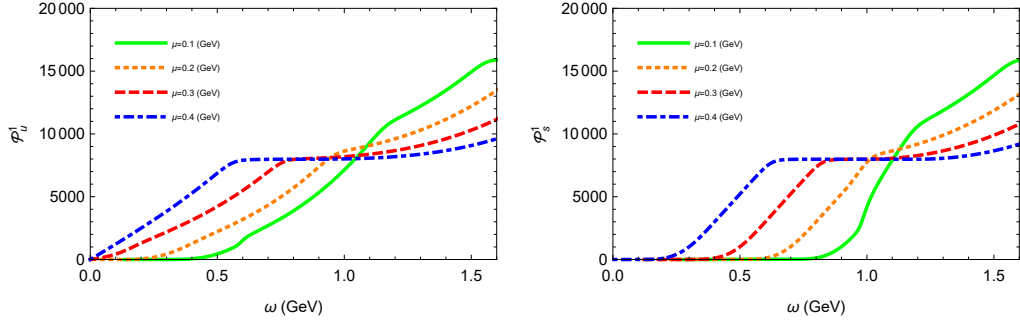


FIG. 8. (Color online) First-order Polarizations of u and s quark as a function of ω for several fixed nonzero values of μ at $T = 0.01$ GeV.

In Fig. 8, the plots of the first-order polarization of u and s quark at $T = 0.01$ GeV are presented for several nonzero chemical potentials, respectively. As is clearly evident, for a given chemical potential the first-order polarization of quarks is found to increase with increase of angular velocity, however, in the case of a large chemical potential is given the first-order polarization is found to slowly varies with the angular velocity that in the middle range of the angular velocity due to at large value of chemical potential the chiral symmetry re-

stored quickly. Comparing the green line in the Fig. 4, it can be seen that the first-order polarizations are affected by the quark nonzero chemical potential which can make the first-order polarization to occur more easily, at $T = 0.01$ GeV the first-order polarizations of u quark and s quark with zero chemical potential start to occur ~ 0.6 GeV and ~ 1.0 GeV, respectively, while that of u quark and s quark with nonzero chemical potential start to occur ~ 0.4 GeV and ~ 0.8 GeV, respectively.

Next, we will analyze the patterns of seconde-order polarization and susceptibility of quark with rotation at nonzero chemical potential. let us firstly consider the effect of angular velocity ω on seconde-order polarization and susceptibility of the quarks at very low temperature. We plot the second-order polarizations and susceptibilities of u and s quark as a function of ω for several fixed nonzero values of chemical potential at $T = 0.01$ GeV in Fig. 9 and Fig. 10, respectively. From the

figures we find the polarization and susceptibility have similar behaviour with respect to angular velocity, so here we only discuss the QNS in detail. we can see if one considers the case of nonzero chemical potential, the behaviour of QNS change considerably and are quite dependent on the angular velocity. From the figure one can see the dependence of QNS on angular velocity is complicated as shown in the figure that the QNS increases with the increasing ω when ω is smaller than

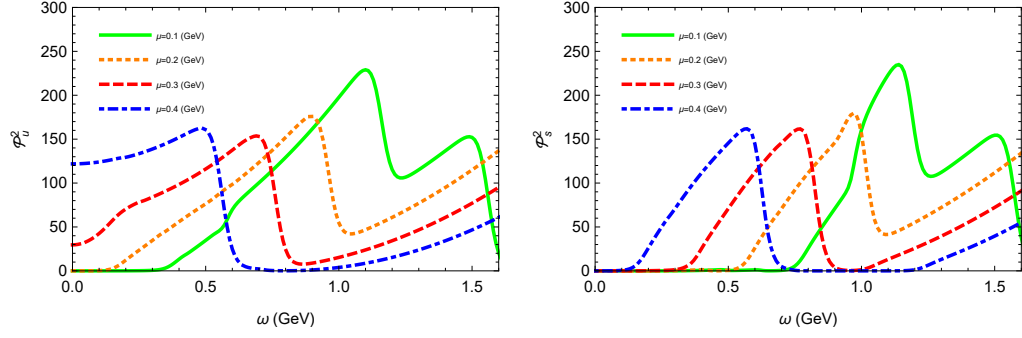


FIG. 9. (Color online) Second-order Polarizations of u and s quark as a function of ω for several fixed nonzero values of μ at $T = 0.01$ GeV.

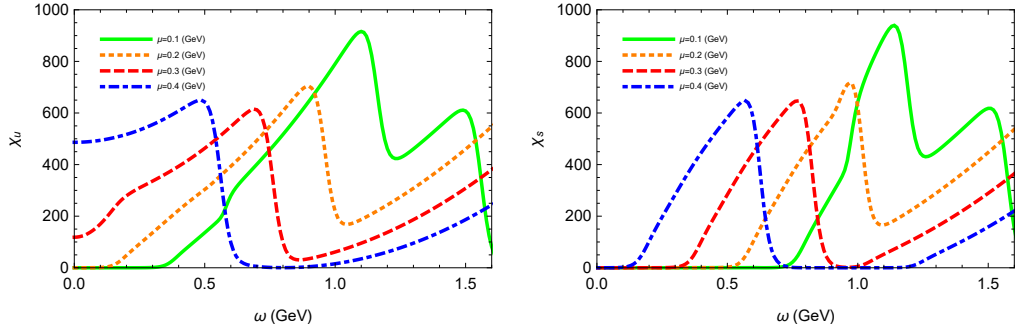


FIG. 10. (Color online) Susceptibilities of u and s quark as a function of ω for several fixed nonzero values of μ at $T = 0.01$ GeV.

a certain value while the QNS decreases with the increasing ω when ω excesses another certain value, which indicates that the rotation matter may provide some new and helpful results to study the phase transition. And there are some interesting changes compare with the situation of zero chemical potential, at $T = 0.01$ GeV the curves of susceptibility of the quark have two peaks, which are very different compared with the green line in Fig. 6, the curves of QNS have such behavior because the gap mass with nonzero chemical potential are dif-

ferent from that the case with zero chemical potential and for any angular velocity which should satisfy the gap equation, whose constraint will have an effect to the susceptibility. In addition, there are some features should be pointed out, for very small or very large angular velocity the chemical potential μ plays an important role to contribute the quark susceptibilities, however with increasing ω , the QNS is changed very considerably.

It may need a bit more explanation about the part played by the angular velocity ω with nonzero chemical potential at high temperature. Fig. 11 shows the mean field mass gap M_u and M_s versus ω with several fixed values of μ , obvi-

ously from the figure we can see there is a generally rotational suppression effect on the scalar paring states just as we point in our precious discussions, however the left panel of the figure shows that at high temperature and with nonzero chemical

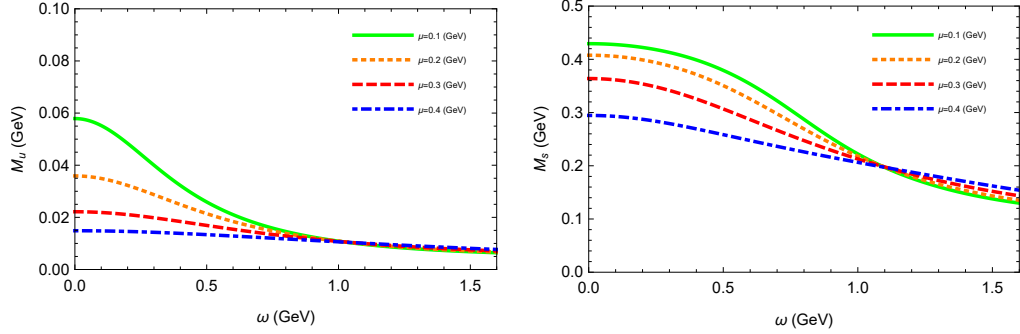


FIG. 11. (Color online) The mean field mass gap M_u and M_s as a function of ω for several fixed values of μ at $T = 0.2$ GeV.

potential the mean field mass gap M_u is not much affected by the rotating, while the right panel of the figure shows that

M_s is much affected due to the current mass of the u quark is very small and whose chiral symmetry can be easily restored compared to that of s quark.

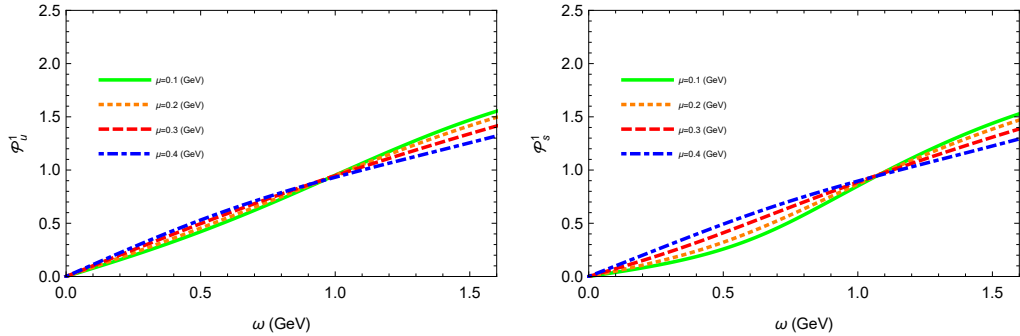


FIG. 12. (Color online) First-order Polarizations of u and s quark as a function of ω for several fixed values of μ at $T = 0.2$ GeV.

In order to see this influence, we plot the first-order polarization of u and s quark as a function of ω for several fixed values of μ with $T = 0.2$ GeV. From Fig. 12, we find that at this temperature the first-order quark spin polarization always occurs with increasing the angular velocity for all the nonzero chemical potential, at large chemical potential, the first-order

polarization of u and s quark increase almost linearly with increasing chemical potential, while at small chemical potential both the u and s quark have a similar behavior, but with a slightly difference in the range $0 \text{ GeV} < \omega < 1.0 \text{ GeV}$, as the chemical potential increases further distinctions between the two have tended to disappear.

Finally we would like to consider the effects of angular ve-

locity ω on seconde-order polarization and susceptibility of

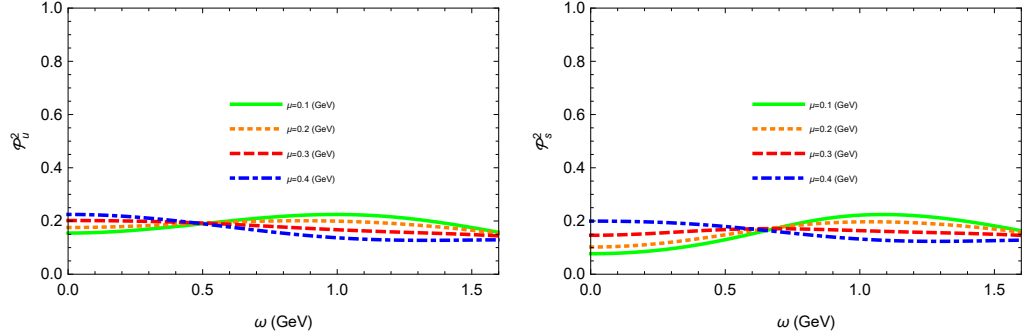


FIG. 13. (Color online) Second-order Polarizations of u and s quark as a function of ω for several fixed nonzero values of μ at $T = 0.2$ GeV.

the quarks at high temperature with several fixed nonzero values of chemical potential and the numerical results are shown in Fig. 13 and Fig. 14. From the figures one immediately makes the following observations: in the case of high temperature ($T = 0.2$ GeV) the variation of seconde-order polarization and susceptibility of the quarks with angular velocity is complicated, we find that at small chemical potential the second-order polarization and susceptibility of the quarks have a peak structure when the chiral phase transition takes place with the increase of angular velocity, when $\omega < 1.0$ GeV at small chemical potential ($\mu = 0.1$ GeV) the second-order polarization or susceptibility of the quarks increases with increase in angular velocity while at large chemical potential ($\mu = 0.4$ GeV) that decreases with increase in angular velocity. It can be also found that at such high temperature the second-order polarization and susceptibility of the quarks can always occur, although the angular velocity suppresses the seconde-order polarization and susceptibility of the quarks in

the range of very large ω . From Fig. 13 and Fig. 14 one could also infer the dependence of the seconde-order polarization and susceptibility of the quarks on the quark current mass when $\omega < 0.5$ GeV is manifest, if the current mass of quark becomes larger, the values of the second-order polarization and susceptibility of the quark become smaller, however with the increasing of ω , the behavior of the both quarks is very similar which means that at high density the large angular velocity takes the predominant role compared to the role played by the temperature and chemical potential. It is very interesting for the behavior of susceptibilities of both u and s quark at the fixed values of the temperature and the angular velocity, from Fig. 14 one can observe that the susceptibilities are quite dependent on the chemical potential μ in the rotation system, at small angular velocity the μ enhances the susceptibilities, and at large angular velocity the chemical potential μ also enhances the susceptibilities.

IV. CONCLUSIONS AND OUTLOOK

Finally, we want to summarize our results and give a brief outlook. In this paper, we have presented detailed analytic formulae for the quark matter under rotation in three-flavor NJL model and related topics have been investigated. In order to have a better understanding of the rotating system with finite density we have also introduced the chemical potential. We studied the quark fields in cylindrical coordinates as well as investigated the effect of the rotating on the quark chiral condensate, quark spin polarization and quark number susceptibility at finite temperature with or without finite chemical potential in this model. We found that the angular velocity plays a very crucial role in these topics, at low temperature, small chemical potential and small angular veloc-

ity, quarks and gluons are confined and chiral symmetry is broken spontaneously, while at large enough angular velocity, deconfinement occurs and chiral symmetry is restored. Our numerical analysis shows that the rotation suppresses the chiral condensation and enhances the first-order quark spin polarization, however for the second-order quark spin polarization and quark number susceptibility the effect is very complicated, which can be found have a peak structure when the first-order phase transitions take place with the increase of angular velocity.

We have also explicitly computed these quantities with nonzero chemical potential, we found that the nonzero chemical potential affects the first-order phase transition and makes the chiral condensate, quark spin polarization and quark number susceptibility have different behaviors. At very low tem-

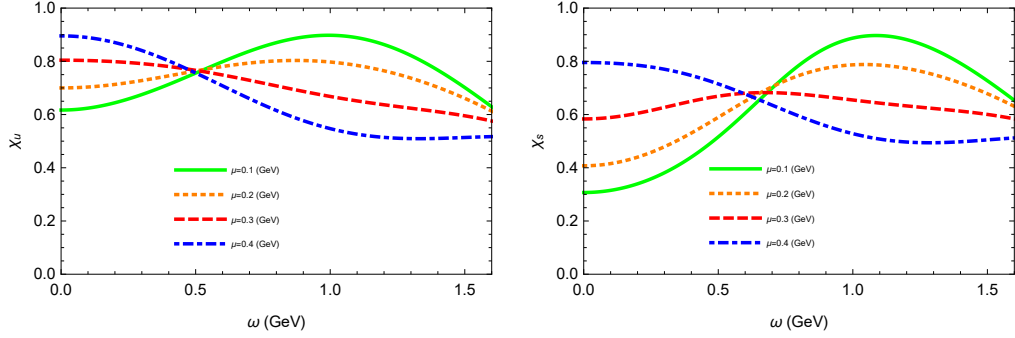


FIG. 14. (Color online) Second-order susceptibilities of u and s quark as a function of ω for several fixed nonzero values of μ at $T = 0.2$ GeV.

perature the chiral condensate experiences a first-order transition when ω exceeds a certain value with zero chemical potential, while at nonzero chemical potential the first-order transition is suppressed and changed to the crossover. It can be also observed that the quark number susceptibilities have two maximum, which indicates that the rotation matter with nonzero chemical potential may provide some new and helpful results to study the phase transition. In this paper we especially considered the contributions from s quark and made some comparisons between u quark and s quark and found that at small angular velocity the part played by current mass to these phenomena is important, however, at sufficiently large angular velocity, the contributions played by different quarks to these phenomena are almost equal. Basing on the interpretations made above, it would be possible to judge and forecast these phenomena of quark matter under rotation in the three-flavor NJL model if we jointly take angular velocity, chemical potential and temperature factors into consideration. We expect these studies to play an important role in help understanding the nature of the critical region in the phase diagram of strongly interacting rotating matter.

The theoretical interest in relativistic rotating systems is being revived in many different physical environments, which is undoubtedly calls for more investigation. For instance, the related effects of rotating fermions inside a cylindrical boundary [110], the investigation of a possible phase structure under rotation including the s quark, especially the exploration to those regions of the phase diagram that cannot be reached on the lattice yet. The NJL model describes only quarks and antiquarks and neglects the gluons, so it is also very worth to extend the rotation system to the Polyakov extended Nambu and Jona-Lasinio (PNJL) model [111], which will consider the complex interactions between quarks and gluons and that the chiral symmetry restoration as well as the effect of quark confinement in PNJL under rotation may provide needed insight into the QCD. This model will have a clearer picture considering the constraint from the experimental related to rotation

conducted at numerous research facilities worldwide as the Brookhaven National Laboratory (BNL), the European Organization for Nuclear Research (CERN) and the GSI Helmholtz Centre for Heavy Ion Research (GSI), due to one can see that some limits can be made for the parameter space under the given assumptions. It would be interesting to use the results obtained in this paper to investigate these topics discussed here, and we leave these as our further study.

ACKNOWLEDGEMENTS

We specially thank Jinfeng Liao for the early involvement in the work and enlightening discussions, and thank Hui Zhang, Akira Watanabe for discussions, corrections and comments. We also thank Shengqin Feng and Yafei Shi for their encouragement and discussions. The work has been supported by the National Natural Science Foundation of China (NSFC) under Grant No. 11647174, No. 11875178, No. 11801311, the Key Laboratory of Quark and Lepton Physics Contracts under Grant No. QLPL201905 and the Science Research Foundation of China Three Gorges University under Grant No. KJ2015A007. AH acknowledges support by the NSF Grant No. PHY1913729 and by the U.S. Department of Energy, Office of Science, Office of Nuclear Physics, within the framework of the Beam Energy Scan Theory (BEST) Topical Collaboration. AH is also grateful to the Fundamental Research Funds for the Central Universities.

Appendix A: The brief description of fermions under rotation

The properties of fermions under global rotation are relevant to a number of problems as discussed above, so it is im-

portant to choose an appropriate complete set of commuting operators in the cylindrical coordinates. In this section, we will start from the Dirac equation in the rotating frame, then we will derive the eigenvectors of the those complete set of

commuting operators.

The general Lagrangian of the rotating fermions is written in the following way [16, 30, 91]

$$\mathcal{L} = \bar{\psi} \left[i\gamma^\mu \partial_\mu - m + (\gamma^0)^{-1} \left((\vec{\omega} \times \vec{x}) \cdot (-i\vec{\partial}) + \vec{\omega} \cdot \vec{S}_{4 \times 4} \right) \right] \psi, \quad (\text{A1})$$

where ψ is the quark field, ω is the angular velocity and m is the bare quark mass matrix, as a result of rotation, we can see the Dirac operator includes the orbit-rotation coupling term

and the spin-rotation coupling term, and we have defined

$$\vec{S}_{4 \times 4} = \frac{1}{2} \begin{pmatrix} \vec{\sigma} & 0 \\ 0 & \vec{\sigma} \end{pmatrix}, \quad (\text{A2})$$

whose z-component related to the spin polarization of the quark. The corresponding Hamiltonian of Eq. (A1) in momentum space reads

$$\hat{\mathcal{H}} = \gamma^0 \left(\vec{\gamma} \cdot \hat{\vec{p}} + m \right) - \vec{\omega} \cdot \left(\vec{x} \times \hat{\vec{p}} + \vec{S}_{4 \times 4} \right) = \hat{\mathcal{H}}_0 + \vec{\omega} \cdot \hat{\vec{J}}, \quad (\text{A3})$$

here

$$\hat{\vec{J}} = \vec{x} \times \hat{\vec{p}} + \vec{S}_{4 \times 4}, \quad (\text{A4})$$

and the first term is the contribution of the angular momentum, the second term is the contribution of the spin angular momentum.

Now considering the energy eigenvalue equation

$$\hat{\mathcal{H}}\psi = E\psi, \quad (\text{A5})$$

here ψ is the four-component spinors and can be written in terms of two-component spinors as

$$\psi = \begin{pmatrix} \phi \\ \chi \end{pmatrix}, \quad (\text{A6})$$

substituting the Hamiltonian above to the energy eigenvalue

equation, then Eq. (A5) transforms simply as

$$\begin{cases} (E - m + \omega_z J_z) \phi = \vec{\sigma} \cdot \hat{\vec{p}} \chi \\ (E + m + \omega_z J_z) \chi = \vec{\sigma} \cdot \hat{\vec{p}} \phi \end{cases} \quad (\text{A7})$$

here,

$$J_z = L_z + \frac{1}{2} \sum_z, \quad (\text{A8})$$

which is the z-component of total angular momentum, then, we consider the z-component angular momentum eigenvalue equation

$$J_z \psi = \left(n + \frac{1}{2} \right) \psi, \quad (\text{A9})$$

after some derivations, we can get the following equation

$$\left(E - m + \omega_z \left(n + \frac{1}{2} \right) \right) \left(E + m + \omega_z \left(n + \frac{1}{2} \right) \right) \phi = \left(\vec{\sigma} \cdot \hat{\vec{p}} \right)^2 \phi, \quad (\text{A10})$$

it is very convenient to make the transform Cartesian coordinate to the Cylindrical coordinate, here separation variable method is applied and ϕ takes the form of

$$\varphi = f(\theta) g(r) h(z), \quad (\text{A11})$$

and the solution for two-component spinors φ in Eqs. (A9) has the form

$$f(\theta) = \begin{pmatrix} e^{in\theta} \\ e^{i(n+1)\theta} \end{pmatrix}, \quad (\text{A12})$$

substituting Eq. (A12) into the Eq. (A10) after some tedious calculations, we find that $g(r)$ satisfies the Bessel-type equation as follows,

$$r^2 \frac{\partial^2 g(r)}{\partial r^2} + r \frac{\partial g(r)}{\partial r} + (r^2 p_t^2 - n^2) g(r) = 0, \quad (\text{A13})$$

$$r^2 \frac{\partial^2 g(r)}{\partial r^2} + r \frac{\partial g(r)}{\partial r} + (r^2 p_t^2 - (n+1)^2) g(r) = 0, \quad (\text{A14})$$

the solutions of Eqs. (A13) and (A14) have the following form, respectively,

$$g(r) = J_n(p_t r), J_{n+1}(p_t r), \quad (\text{A15})$$

where J is the Bessel function. In order to commute with

other operators we must define the helicity operator, the general helicity operator has the following form

$$h_t = \gamma^5 \cdot \gamma^3 \frac{\vec{\sum} \cdot \vec{p}_t}{|\vec{p}_t|} = \frac{1}{i|\vec{p}_t|} \begin{pmatrix} 0 & -P_- & 0 & 0 \\ P_+ & 0 & 0 & 0 \\ 0 & 0 & 0 & P_- \\ 0 & 0 & -P_+ & 0 \end{pmatrix}, \quad (\text{A16})$$

here, p_t is the transverse momentum, $P_+ = \hat{p}_x + i\hat{p}_y$, $P_- = \hat{p}_x - i\hat{p}_y$ and in Cylindrical coordinates they have such forms

$$P_+ = -ie^{i\theta} \left(\frac{\partial}{\partial r} + i\frac{1}{r} \frac{\partial}{\partial \theta} \right), \quad (\text{A17})$$

$$P_- = -ie^{-i\theta} \left(\frac{\partial}{\partial r} - i\frac{1}{r} \frac{\partial}{\partial \theta} \right), \quad (\text{A18})$$

which like shift operators when act on the terms including angular momentum quantum number $e^{in\theta} J_n(p_t r)$, $e^{i(n+1)\theta} J_{n+1}(p_t r)$, respectively, they satisfy the following relationship

$$P_+ e^{in\theta} J_n(p_t r) = ip_t e^{i(n+1)\theta} J_{n+1}(p_t r), \quad (\text{A19})$$

$$P_- e^{i(n+1)\theta} J_{n+1}(p_t r) = -ip_t e^{in\theta} J_n(p_t r). \quad (\text{A20})$$

Reconsidering the transverse helicity equation and the generalized orthogonality relation

$$h_t \psi = s \psi, \quad (\text{A21})$$

$$\sum_{n=-\infty}^{\infty} \psi^\dagger \psi = 1, \quad (\text{A22})$$

here, $s = \pm 1$ represent the transverse helicity, the solutions of the positive energy eigenvalues are obtained as follows

$$u = \frac{1}{\sqrt{2}} \begin{pmatrix} e^{ip_z z} e^{in\theta} J_n(p_t r) \\ se^{ip_z z} e^{i(n+1)\theta} J_{n+1}(p_t r) \\ e^{ip_z z} e^{in\theta} J_n(p_t r) \\ se^{ip_z z} e^{i(n+1)\theta} J_{n+1}(p_t r) \end{pmatrix}, \quad (\text{A23})$$

where, u is a four-component spinor which must satisfy the Dirac equation

$$(i\gamma^\mu \partial_\mu - m)u = 0, \quad (\text{A24})$$

substituting u into the Dirac equation gives

$$\begin{pmatrix} E - m & -\sigma.p \\ \sigma.p & -E - m \end{pmatrix} \begin{pmatrix} c_A u_A \\ c_B u_B \end{pmatrix} = 0, \quad (\text{A25})$$

here u_A, u_B are two-component spinors and c_A, c_B are normalization constants, after some calculations we get

$$c_B u_B = c_A \begin{pmatrix} \frac{(p_z - isp_t)}{E+m} e^{ip_z z} e^{in\theta} J_n(p_t r) \\ \frac{(-sp_z + ip_t)}{E+m} e^{ip_z z} e^{i(n+1)\theta} J_{n+1}(p_t r) \end{pmatrix}, \quad (\text{A26})$$

imposing the generalized completeness relation

$$\sum_{n=-\infty}^{\infty} u^\dagger u = 1, \quad (\text{A27})$$

these constant factors can be determined and finally we ob-

tain the positive energy particle solutions with positive and

negative helicity in the Dirac representation, which take the following explicit form

$$u = \frac{1}{2} \sqrt{\frac{E+m}{E}} \begin{pmatrix} e^{ip_z z} e^{in\theta} J_n(p_t r) \\ se^{ip_z z} e^{i(n+1)\theta} J_{n+1}(p_t r) \\ \frac{p_z - is p_t}{E+m} e^{ip_z z} e^{in\theta} J_n(p_t r) \\ \frac{-sp_z + ip_t}{E+m} e^{ip_z z} e^{i(n+1)\theta} J_{n+1}(p_t r) \end{pmatrix}, \quad (\text{A28})$$

in exactly the same way, the negative-energy antiparticle so-

lutions are listed below

$$v = \frac{1}{2} \sqrt{\frac{E+m}{E}} \begin{pmatrix} \frac{p_z - is p_t}{E+m} e^{-ip_z z} e^{in\theta} J_n(p_t r) \\ \frac{-sp_z + ip_t}{E+m} e^{-ip_z z} e^{i(n+1)\theta} J_{n+1}(p_t r) \\ e^{-ip_z z} e^{in\theta} J_n(p_t r) \\ -se^{-ip_z z} e^{i(n+1)\theta} J_{n+1}(p_t r) \end{pmatrix}. \quad (\text{A29})$$

- [1] D. Kharzeev and A. Zhitnitsky, Nucl. Phys. A797, 67 (2007).
- [2] D.T. Son and P. Surowka, Phys. Rev. Lett. 103, 191601 (2009).
- [3] D.E. Kharzeev and D. T. Son, Phys. Rev. Lett. 106, 062301 (2011).
- [4] Y. Jiang, X. G. Huang, and J. Liao, Phys. Rev. D 92, 071501 (2015).
- [5] Kharzeev, D. E., Liao, J., Voloshin, S. A. & Wang, G. Chiral magnetic and vortical effects in high-energy nuclear collisionsA status report. Prog. Part. Nucl. Phys. 88, 1-28 (2016). 1511.04050.
- [6] L.P. Csernai, V.K. Magas and D.J. Wang, Phys. Rev. C 87, no. 3, 034906 (2013).
- [7] F. Becattini et al., Eur. Phys. J. C 75, no. 9, 406 (2015).
- [8] Y. Jiang, Z.W. Lin and J. Liao, Phys. Rev. C 94, no. 4, 044910 (2016) Erratum: [Phys. Rev. C 95, no. 4, 049904 (2017)].
- [9] S. Shi, K. Li and J. Liao, Phys. Lett. B 788, 409 (2019).
- [10] W.T. Deng and X.G. Huang, Phys. Rev. C 93, no. 6, 064907 (2016).
- [11] L.G. Pang, H. Petersen, Q. Wang and X.N. Wang, Phys. Rev. Lett. 117, no. 19, 192301 (2016).
- [12] L. Adamczyk et al. [STAR Collaboration], Nature 548, 62 (2017) doi:10.1038/nature23004 [arXiv:1701.06657 [nucl-ex]].
- [13] F. Becattini, I. Karpenko, M. Lisa, I. Upsal and S. Voloshin, Phys. Rev. C 95, no. 5, 054902 (2017).
- [14] X.L. Xia, H.Li, Z.B. Tang and Q. Wang, Phys. Rev. C 98, 024905 (2018).
- [15] Hui Zhang, Defu Hou and Jinfeng Liao, arXiv:1812.11787v3 [hep-ph].
- [16] A.L. Fetter, Rev. Mod. Phys. 81, 647 (2009). doi:10.1103/Rev Mod Phys. 81. 647.
- [17] Urban, M., Schuck, P. 2008, Phys. Rev. A , 78, 011601.
- [18] Iskin, M., Tiesinga, E. 2009, Phys. Rev. A , 79, 053621.
- [19] R. Takahashi, et al, Nature Physics volume 12 (2016).
- [20] J. Gooth et al., Nature 547, 324 (2017).
- [21] A. Vilenkin, Parity Violating Currents in Thermal Radiation, Phys. Lett. 80B (1978) 150.
- [22] A. Vilenkin, Macroscopic Parity Violating Effects: Neutrino Fluxes From Rotating Black Holes And In Rotating Thermal Radiation, Phys. Rev. D 20 (1979) 1807 [INSPIRE].
- [23] A. Vilenkin, Quantum Field Theory At Finite Temperature In A Rotating System, Phys. Rev. D 21 (1980) 2260 [INSPIRE].
- [24] M. Kaminski, C.F. Uhlemann, M. Bleicher and J. Schaffner-Bielich, Anomalous hydrodynamics kicks neutron stars, Phys. Lett. B 760 (2016) 170 [arXiv:1410.3833] [INSPIRE].
- [25] N. Yamamoto, Chiral transport of neutrinos in supernovae: Neutrino-induced uid helicity and helical plasma instability, Phys. Rev. D 93 (2016) 065017 [arXiv:1511.00933] [INSPIRE].
- [26] E. Shaverin and A. Yarom, An anomalous propulsion mechanism, arXiv:1411.5581 [INSPIRE].
- [27] A. L. Watts et al., Rev. Mod. Phys. 88, no. 2, 021001 (2016) doi:10.1103/Rev Mod Phys. 88. 021001 [arXiv:1602.01081 [astro-ph.HE]].
- [28] I. A. Grenier and A. K. Harding, Comptes Rendus Physique 16, 641 doi: 10.1016/j.crhy.2015.08.013 [arXiv:1509.08823 [astro-ph.HE]].
- [29] E. Berti, F. White, A. Maniopoulou and M. Bruni, Mon. Not. Roy. Astron. Soc. 358, 923 (2005) doi:10.1111/j.1365-2966.2005.08812.x [gr-qc/0405146].
- [30] A. Yamamoto and Y. Hirono, Phys. Rev. Lett. 111, 081601 (2013) doi:10.1103/Phys. Rev. Lett. 111. 081601 [arXiv:1303.6292 [hep-lat]].
- [31] Z.T. Liang and X.N. Wang, "Globally Polarized Quark Gluon Plasma in Noncentral A+A Collisions," Phys. Rev. Lett. 94, 102301 (2005), [Erratum: Phys. Rev. Lett. 96, 039901 (2006)].
- [32] Sergei A. Voloshin, "Polarized secondary particles in unpolarized high energy hadron-hadron collisions?" (2004), arXiv:nucl-th/0410089 [nucl-th].

[33] F. Becattini, F. Piccinini, and J. Rizzo, "Angular momentum conservation in heavy ion collisions at very high energy," *Phys. Rev. C* 77, 024906 (2008).

[34] Z.T. Liang and X. N. Wang, *Phys. Rev. Lett.* 94 (2005) 102301, nuclth/0410079, [Erratum: *Phys. Rev. Lett.* 96, 039901 (2006)].

[35] X.G. Huang, P. Huovinen and X.N. Wang, *Phys. Rev. C* 84 (2011) 054910, 1108.5649.

[36] X.G. Huang, *Rept. Prog. Phys.* 79 (2016) 076302, 1509.04073.

[37] F. Becattini and F. Piccinini, *Ann. Phys. (Amsterdam)* 323 (2008) 2452 .

[38] F. Becattini et al., *Ann. Phys. (Amsterdam)* 338 (2013) 32 .

[39] F. Becattini et al., *Eur. Phys. J.* C75 (2015) 406, 1501.04468.

[40] A. Aristova et al., (2016), 1606.05882.

[41] W.T. Deng and X.G. Huang, *Phys. Rev. C* 93 (2016) 064907, 1603.06117.

[42] Shu Ebihara, Kenji Fukushima, Kazuya Mameda, *Phys. Lett. B* 764, 10 (2017).

[43] L. Adamczyk et al. [STAR], *Nature* 548, 62-65 (2017) [arXiv:1701.06657 [nucl-ex]].

[44] J. Adam et al. [STAR], *Phys. Rev. C* 98, 014910 (2018) [arXiv:1805.04400 [nucl-ex]].

[45] S. Acharya et al. [ALICE], *Phys. Rev. C* 101, 044611 (2020) [arXiv:1909.01281 [nucl-ex]].

[46] Y. Tsue, J. da Providência, C. Providência, M. Yamamura, and H. Bohr, *Prog. Theor. Exp. Phys.* 2013, 103D01 (2013).

[47] Y. Tsue, J. da Providência, C. Providência, M. Yamamura, and H. Bohr, *Prog. Theor. Exp. Phys.* 2015, 103D02 (2015).

[48] Y. Tsue, J. da Providência, C. Providência, M. Yamamura, and H. Bohr, *Prog. Theor. Exp. Phys.* 2015, 103D01 (2015).

[49] H. Matsuoka, Y. Tsue, J. da Providência, C. Providência, M. Yamamura, and H. Bohr, *Prog. Theor. Exp. Phys.* 2016, 053D02 (2016).

[50] H. Matsuoka, Y. Tsue, J. da Providência, M. Yamamura, *Phys. Rev. D* 95, 054025 (2017).

[51] X. G. Huang, J. Liao, Q. Wang, and X. L. Xia, Vorticity and spin polarization in heavy ion collisions: Transport models, arXiv:2010.08937.

[52] F. Becattini and M.A. Lisa, Polarization and Vorticity in the quark gluon plasma, *Annu. Rev. Nucl. Part. Sci.* 70, 395 (2020).

[53] S. Jeon and V. Koch, Event by event fluctuations, in Quark gluon plasma, R.C. Hwa and X.N. Wang eds., World Scientific, pp. 430-490 [hep-ph/0304012] [INSPIRE].

[54] V. Koch, Hadronic fluctuations and correlations, arXiv:0810.2520 [INSPIRE].

[55] A. Bzdak, V. Koch and J. Liao, Remarks on possible local parity violation in heavy ion collisions, *Phys. Rev. C* 81 (2010) 031901 [arXiv:0912.5050] [INSPIRE].

[56] STAR collaboration, X.-F. Luo, Probing the QCD critical point with higher moments of net-proton multiplicity distributions, *J. Phys. Conf. Ser.* 316 (2011) 012003 [arXiv:1106.2926] [INSPIRE].

[57] S. Gupta, X. Luo, B. Mohanty, H.G. Ritter and N. Xu, Scale for the phase diagram of quantum chromodynamics, *Science* 332 (2011) 1525 [arXiv:1105.3934] [INSPIRE].

[58] A. Bzdak, V. Koch and J. Liao, Charge-dependent correlations in relativistic heavy ion collisions and the chiral magnetic effect, *Lect. Notes Phys.* 871 (2013) 503 [arXiv:1207.7327] [INSPIRE].

[59] A. Bazavov et al., Freeze-out conditions in heavy ion collisions from QCD thermodynamics, *Phys. Rev. Lett.* 109 (2012) 192302 [arXiv:1208.1220] [INSPIRE].

[60] X.F. Luo, B. Mohanty, H.G. Ritter and N. Xu, Search for the QCD critical point: higher moments of net-proton multiplicity distributions, *Phys. Atom. Nucl.* 75 (2012) 676 [arXiv:1105.5049] [INSPIRE].

[61] X. Luo, J. Xu, B. Mohanty and N. Xu, Techniques in the moment analysis of net-proton multiplicity distributions in heavy-ion collisions, arXiv:1302.2332 [INSPIRE].

[62] STAR collaboration, X. Luo, Search for the QCD critical point by higher moments of net-proton multiplicity distributions at STAR, *Nucl. Phys. A* 904-905 (2013) 911c-914c [arXiv:1210.5573] [INSPIRE].

[63] Shuzhe Shi and Jinfeng Liao, 10.1007/JHEP 06 (2013) 104.

[64] R. V. Gavai and S. Gupta, *Phys. Rev. D* 68 (2003) 034506.

[65] R. V. Gavai and S. Gupta, *Phys. Rev. D* 71 (2005) 114014.

[66] S. Gupta, N. Karthik and P. Majumdar, *Phys. Rev. D* 90 (2014) 034001.

[67] L. Adamczyk et al., (STAR Collaboration), *Phys. Rev. Lett.* 112, 032302 (2014).

[68] L. Adamczyk et al., (STAR Collaboration), *Phys. Rev. Lett.* 113, 092301 (2014).

[69] X. Luo, *EPJ Web of Conferences*, 141.04001 (2017).

[70] R. Gavai and S. Gupta, "Fluctuations, strangeness and quasi-quarks in heavy-ion collisions from lattice QCD," *Phys. Rev. D* 73, 014004 (2006).

[71] S. Borsanyi, Z. Fodor, S. Katz, S. Krieg, C. Ratti and K. Szabo, "Freeze-out parameters: lattice meets experiment," *Phys. Rev. Lett.* 111, 062005 (2013).

[72] S. Borsanyi, "Thermodynamics of the QCD transition from lattice," *Nucl. Phys. A* 904-905, 270c-277c (2013).

[73] R. Bellwied, S. Borsanyi, Z. Fodor, S. Katz, A. Pasztor, C. Ratti and K. Szabo, "Fluctuations and correlations in high temperature QCD," *Phys. Rev. D* 92, no.11, 114505 (2015).

[74] H.T. Ding, S. Mukherjee, H. Ohno, P. Petreczky and H.P. Schadler, "Diagonal and off-diagonal quark number susceptibilities at high temperatures," *Phys. Rev. D* 92, no.7, 074043 (2015).

[75] T. Kunihiro, *Phys. Lett. B* 271 (1991) 395.

[76] H. Fujii and M. Ohtani, *Phys. Rev. D* 70 (2004) 014016.

[77] Y. Hatta and T. Ikeda, *Phys. Rev. D* 67 (2003) 014028.

[78] B.J. Schaefer and J. Wambach, *Phys. Rev. D* 75 (2007) 085015.

[79] A.R. Bodmer, *Phys. Rev. D* 4 (1971) 1601.

[80] E. Witten, *Phys. Rev. D* 30 (1984) 272.

[81] C. Alcock, E. Farhi, and A.V. Olinto, *Astrophys. J.* 310 (1986) 261.

[82] C. Alcock and A.V. Olinto, *Ann. Rev. Nucl. Part. Sci.* 38 (1988) 161.

[83] J. Madsen, *Lecture Notes in Physics* 516 (1999) 162.

[84] N.K. Glendenning and F. Weber, *Astrophys. J.* 400 (1992) 647.

[85] N.K. Glendenning, Ch. Kettner, and F. Weber, *Astrophys. J.* 450 (1995) 253.

[86] N.K. Glendenning, Ch. Kettner, and F. Weber, *Phys. Rev. Lett.* 74 (1995) 3519

[87] H. Terazawa, INS-Report-338 (INS, Univ. of Tokyo, 1979).

[88] H. Terazawa, *J. Phys. Soc. Jpn.* 58 (1989) 3555.

[89] H. Terazawa, *J. Phys. Soc. Jpn.* 58 (1989) 4388.

[90] H. Terazawa, *J. Phys. Soc. Jpn.* 59 (1990) 1199.

[91] Y. Jiang and J. Liao, *Phys. Rev. Lett.* 117, 192302 (2016).

[92] M. Buballa, *Phys. Rept.* 407, 205 (2005).

[93] J. I. Kapusta, *Finite Temperature Field Theory* (Cambridge University Press, Cambridge, England, 1989).

[94] F. Becattinia, F. Piccinini *Annals of Physics* 323 (2008) 2452-2473.

- [95] R.V. Gavai and S. Gupta, Pressure and nonlinear susceptibilities in QCD at finite chemical potentials, *Phys. Rev. D* 68 (2003) 034506 [[hep-lat/0303013](#)] [[INSPIRE](#)].
- [96] R.V. Gavai and S. Gupta, Simple patterns for non-linear susceptibilities near T_c , *Phys. Rev. D* 72 (2005) 054006 [[hep-lat/0507023](#)] [[INSPIRE](#)].
- [97] R.V. Gavai and S. Gupta, The critical end point of QCD, *Phys. Rev. D* 71 (2005) 114014 [[hep-lat/0412035](#)] [[INSPIRE](#)].
- [98] C.R. Allton et al., Thermodynamics of two flavor QCD to sixth order in quark chemical potential, *Phys. Rev. D* 71 (2005) 054508 [[hep-lat/0501030](#)] [[INSPIRE](#)].
- [99] M. Cheng et al., Baryon number, strangeness and electric charge fluctuations in QCD at high temperature, *Phys. Rev. D* 79 (2009) 074505 [[arXiv:0811.1006](#)] [[INSPIRE](#)].
- [100] S. Borsányi et al., Fluctuations of conserved charges at finite temperature from lattice QCD, *JHEP* 01 (2012) 138 [[arXiv:1112.4416](#)] [[INSPIRE](#)].
- [101] HotQCD collaboration, A. Bazavov et al., Fluctuations and correlations of net baryon number, electric charge and strangeness: a comparison of lattice QCD results with the hadron resonance gas model, *Phys. Rev. D* 86 (2012) 034509 [[arXiv:1203.0784](#)] [[INSPIRE](#)].
- [102] H.L. Chen, K. Fukushima, X. G. Huang, and K. Mameda, *Phys. Rev. D* 93, 104052 (2016).
- [103] S. Ebihara, K. Fukushima, and K. Mameda, *Phys. Lett. B* 764, 94 (2017).
- [104] M.N. Chernodub and S. Gongyo, *J. High Energy Phys.* 01 (2017) 136 [[arXiv:1611.02598](#)] [[INSPIRE](#)].
- [105] M.N. Chernodub and S. Gongyo, *Phys. Rev. D* 95, 096006 (2017).
- [106] M.N. Chernodub, Inhomogeneous confining-deconfining phases in rotating plasmas, *Phys. Rev. D* 103, 054027 (2021) [[arXiv:2012.04924](#)] [[INSPIRE](#)].
- [107] Xinyang Wang, Minghua Wei, Zhibin Li and Mei Huang, Quark matter under rotation in the NJL model with vector interaction, *Phys. Rev. D* 99, 016018 (2019).
- [108] H. Kohyama, D. Kimura, T. Inagaki, *Nuclear Physics B* 906(2016) 524-548.
- [109] S.P. Klevansky, *Rev. Mod. Phys.* 64, 649 (1992).
- [110] Victor E. Ambrus, Elizabeth Winstanley, *Phys. Rev. D* 93, 104014 (2016).
- [111] C. Ratti, M.A. Thaler and W. Weise, *Phys. Rev. D* 73, 014019 (2006).